

# Single-cell-gap transfective liquid-crystal display and the use of photoalignment technology

Tao Du  
Lishuang Yao  
Vladimir G. Chigrinov  
Hoi-sing Kwok

**Abstract** — In this paper, transfective liquid-crystal-display (LCD) technology will be reviewed, and several new single-cell-gap transfective LCD configurations are proposed. Photoalignment technology is studied especially for transfective-LCD applications. In order to realize the optimal performance of the display as well as a matched transmittance/reflectance voltage curve (TVC/RVC) for the transfective configurations, two different single-cell-gap transfective-LCD approaches will be discussed. The first one is the dual-mode single-cell-gap approach, in which different liquid-crystal modes are applied to the transmissive and reflective subpixels of the transfective LCD. The other approach is the single-mode single-cell-gap approach, in which an in-cell retardation film is applied to adjust the performance and TVC/RVC matching of a transfective LCD. Photoalignment technology is used to fabricate the dual-mode liquid-crystal cell in the first approach and also the in-cell retardation film in the second approach. Prototypes of the proposed configurations have been fabricated, which show good performance and a matched TVC/RVC.

**Keywords** — *Transfective, photoalignment, self-align, in-cell retardation film.*

DOI # 10.1889/JSID18.6.421

## 1 Introduction

The transmissive LCD is mainstream in the display market. Because it has been under developed for many years, high-level transmissive LCDs exhibit high contrast, high brightness, wide viewing angle, and fast response in indoor environments; however, in outdoor environment, the display performance suffers under strong ambient light. In this circumstance, reflective LCDs will show superior image quality because they make use of the ambient light as the light source. For mobile and portable applications, a combination of indoor and outdoor performance is required; thus, transfective LCDs have entered the market and have found many applications in mobile and portable electronic devices such as mobile phones, e-books, personal digital assistants (PDAs), and portable media players.<sup>1</sup>

Transfective LCDs were first demonstrated in 1978 by J. B. Bigelow, who inserted a translector under the rear polarizer of a conventional LCD configuration, which made the display partially transmissive and partially reflective.<sup>2</sup> A lot of simple transfective displays have been produced based on this simple idea. Unfortunately, the parallax-effect problem prevented this technology from being used in many applications. Low reflectance was another problem because light has to pass through the polarizer four times in the reflective mode.<sup>3</sup> Later, in an optimized transfective configuration, the translector was moved to the inner side of the rear glass, thus the parallax-effect and the low-reflectance problems were solved. However, the mismatch of the TVC and the RVC, which is caused by the different retardations of the light path through the transmissive and reflec-

tive parts of the liquid-crystal cell,<sup>3</sup> made it unsuitable for TFT-LCD applications because the same gray scale cannot be generated by the same voltage applied to both the reflective and transmissive modes.

To solve the mismatching problem, some companies such as Sharp and LG. Philips proposed double-cell-gap configurations. For the double-cell-gap approach, the pixels are separated into transmissive and reflective subpixels. The transmissive subpixels in a transfective display transmit backlight illumination, and the reflective subpixels reflect light from the environment under ambient illumination. The cell gap of the reflective subpixels is made to be approximately half of the transmissive subpixels, so that the light path of both the transmissive and reflective subpixels will be the same.<sup>4</sup> Given the same retardation in both parts, a good match of TVC/RVC could be obtained. The output light intensities in both the transmissive and reflective parts are high because full optimization can be achieved simultaneously for both parts. Several optical modes such as twisted nematic (TN), fringe field switching (FFS), hybrid-aligned nematic (HAN), optically compensated bend (OCB), and in-plane switching (IPS) have been applied in double-cell-gap-configuration transfective LCDs.<sup>5,8</sup> However, the double-cell-gap structure needs special treatment on the glass substrate, which results in high complexity in the fabrication process. It is not advantageous to use transfective LCDs in portable devices because of their high production cost. Figure 1 shows the double-cell-gap configurations proposed by Sharp and LG. Philips.

Alternatively, various single-cell-gap transfective LCDs using patterned indium tin oxide (ITO) electrodes in

Received 08/14/2009; accepted 03/16/2010.

The authors are with the Center for Display Research, Hong Kong University of Science and Technology, Department of Electronic and Computer Engineering, Clear Water Bay, Kowloon 00852, Hong Kong; telephone +852-235-88843, e-mail: ddtao@ust.hk.

© Copyright 2010 Society for Information Display 1071-0922/10/1806-0421\$1.00.

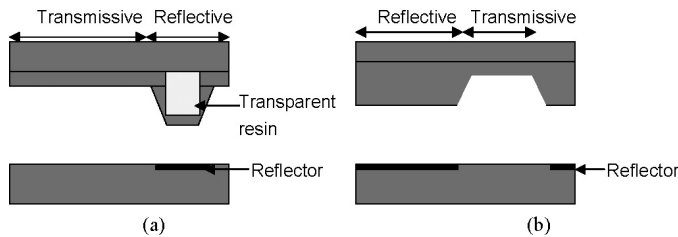


**FIGURE 1** — Dual-cell-gap configurations proposed by (a) Sharp and (b) LG Philips.

the transmissive and reflective regions have been proposed.<sup>9,12</sup> Figure 2 shows a schematic of the patterned ITO in the transmissive and reflective parts. In such an approach, transmissive and reflective parts have the same cell gap but different ITO patterns. Patterned ITO structures result in different voltages for the transmissive and reflective parts, respectively, giving rise to the same retardation in both parts. However, patterned ITO also brings high complexity into the fabrication process.

## 2 Background

Recently, many efforts have been put into the study of single-cell-gap transfective LCDs using the conventional fabrication technique. The basic concepts can be classified into two approaches. For the first approach, which we call the dual-mode single-cell-gap approach, each pixel of the transfective LCD is divided into two subpixels: the transmissive subpixel and reflective subpixel, which have different liquid-crystal modes produced by special alignment technology.<sup>13,18</sup> The LC operation modes for two subpixels are designed to be different so that each mode can be optimized for each part, respectively. High light efficiency can be achieved simultaneously for both parts, and a good match of TVC/RVC can be realized. In the second approach, which we call the single-mode single-cell-gap approach, transmissive and reflective subpixels may still exist, but the liquid-crystal modes in both subpixels are the same. So, there is no need for special treatment of the alignment layer, but in-cell retardation film is required to help adjust the performance of both the transmissive and reflective parts of the transfective LCD. A good match of TVC/RVC can also be realized with the help of in-cell retardation film. Several new trans-

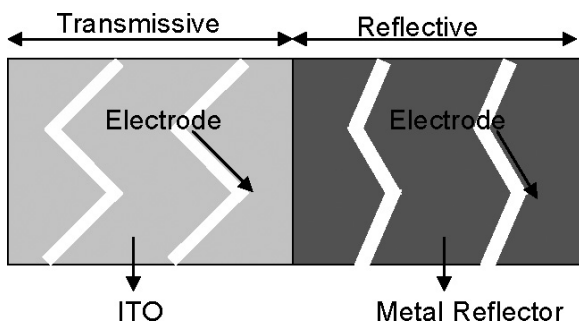


**FIGURE 2** — Schematic of the patterned ITO in the transmissive and reflective parts.

fective configurations based on the two approaches is proposed in this paper.

The photoalignment technique is a new method of alignment-layer treatment that is currently being pursued by many research and industry groups. It is usually performed by shining a polarized UV light to cure the “raw” polyimide or activate the azo-dye molecules. The liquid-crystal molecule, after filling, will align either parallel or perpendicular to the UV light polarization during the treatment, depending on the material. The photoalignment technique proves to possess many advantages in comparison with the usually applied rubbing treatment of the substrates. The benefits for using such a technique are to avoid electrostatic charges and impurities on the polyimide substrate. Moreover, photoalignment technology can be used to fabricate structures with the required liquid-crystal alignment within the selected area of the cell, thus allowing pixel dividing of the domain structure.<sup>19,20</sup>

Photoalignment technology can find very important applications in both of the two new transfective-LCD approaches. In our group, we apply photoalignment technology to the fabrication of patterned liquid-crystal alignment of the dual-mode approach, as well as in the fabrication of in-cell retardation film of the single-mode approach. The fabrication processes will also be discussed in this paper.

## 3 Dual-mode single-cell-gap approach

In the dual-mode single-cell-gap transfective-LCD configurations, different liquid-crystal modes can be applied to the transmissive and reflective subpixels of the display. Ideally, all conventional liquid-crystal modes can be applied and adjusted in this approach, including ECB, TN, OCB, VAN, and IPS.

Here, we introduce one dual-mode transfective configuration proposed in our group, which is called a LTN-TN configuration. In this configuration, the TN mode is applied in the transmissive part and the low-twisted nematic (LTN) mode is applied in the reflective part.

In order to make the simulation more realistic, the LC material we chose is ZLI-4792 from E. Merck in all our simulation process. The ordinary refractive index and extraordinary refractive index for ZLI-4792 are  $n_o = 1.4939$  and  $n_e = 1.5987$ ,  $n_o = 1.4819$  and  $n_e = 1.5809$ , and  $n_o = 1.4774$  and  $n_e = 1.5734$  for a wavelengths of 436, 546, and 633 nm, respectively. The dielectric anisotropy and the elastic constants are  $\Delta\epsilon = 5.2$ ,  $K_1 = 1.32 \times 10^{-6}$ ,  $K_2 = 6.5 \times 10^{-7}$ , and  $K_3 = 1.38 \times 10^{-6}$  dyne, respectively. The cell gap for both the transmissive and reflective parts is 5  $\mu\text{m}$ . The surface pretilt angle is 2° for both the transmissive and reflective parts. The light source used in simulation is D65, ranging from 380 to 720 nm. The absorption and dispersion of the polarizer and compensation films are also considered in this simulation.

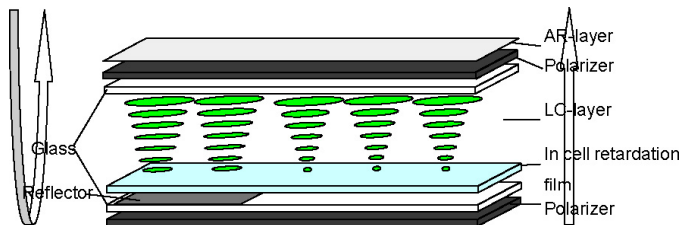


FIGURE 3 — Schematic diagram of the LTN-TN configuration.

### 3.1 LTN-TN configuration

Figure 3 shows the schematic diagram of the LTN-TN configuration. Similar to conventional transfective LCDs, in this dual-mode configuration, each pixel is divided into reflective and transmissive subpixels. The liquid crystal in the reflective subpixel is twisted by  $40^\circ$ , while the liquid crystal in the transmissive subpixel is twisted to  $90^\circ$ . An ordinary polarizer coated with an antireflective layer is applied to the front of the configuration to lower the surface reflection. The in-cell retardation film as well as the patterned reflector is produced on the rear glass. The optimized parameters are shown in Table 1. The angle indicates the counter-clockwise value relative to the horizontal axis.

Figure 4 shows the simulation performance of the LTN-TN transfective LCD: (a) shows the spectrum of the reflective part, (b) the spectrum of the transmissive part, (c) the contrast-ratio distribution of the reflective part, (d) the contrast-ratio distribution of the transmissive part, (e) the simulated TVC and RVC, (f) the experimental results of the TVC and RVC. For the reflective part, the reflectance is 60% of the polarized light, and the maximum contrast is 80%. For the transmissive part, the transmittance is 74% of the polarized light, and the maximum contrast is 15 taking into consideration all the reflection from each layer. The experimental results confirmed that the TVC and RVC match very well. Figure 5 shows the prototype made in the Center for Display Research (CDR).

### 3.2 Single-mode single-cell-gap approach

To make a transfective LCD by using the single-mode single-cell-gap approach, usually we still need to divide each pixel into reflective and transmissive subpixels, but the patterned alignment layer of the cell is not necessary. Instead, we use an in-cell retardation film, which can be adjusted to help optimize the reflective and the transmissive parts of the display. The in-cell retardation film can be a uniform film with a controllable thickness, and it can also be a patterned film

TABLE 1 — Optimized parameters of the transfective LCD.

| Parameter                                     | Transmissive    | Reflective      |
|---|-----------------|-----------------|
| Top polarizer orientation                     | $90^\circ$      | $90^\circ$      |
| LC twist angle                                | $90^\circ$      | $40^\circ$      |
| Cell gap                                      | $5 \mu\text{m}$ | $5 \mu\text{m}$ |
| In-cell retardation film (132 nm) orientation | $88^\circ$      | $88^\circ$      |
| Bottom polarizer orientation                  | $90^\circ$      | —               |

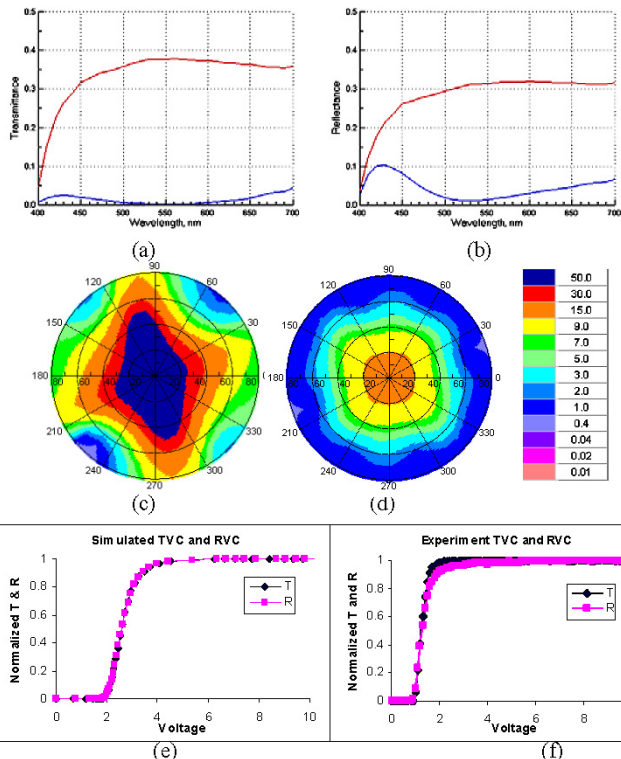


FIGURE 4 — Simulation performance of the LTN-TN transfective LCD. (a) Spectrum of the reflective part, (b) spectrum of the transmissive part, (c) contrast-ratio distribution of the reflective part, (d) contrast-ratio distribution of the transmissive part, (e) simulated TVC and RVC, (f) experiment results of the TVC and RVC.

with different orientations of the reflective and transmissive subpixels. Photoalignment technology is used to fabricate the in-cell retardation films.

Here, we introduce one single-mode configuration proposed by our group, which is called a TN $90^\circ$  configuration. In this configuration, a TN mode with a  $90^\circ$  twist angle is applied to the whole liquid-crystal cell, and two patterned in-cell retardation films are used to adjust the performance of the display.

In the simulation, all the liquid-crystal parameters are the same for the LTN-TN configuration, making the simulation more realistic.

### 4.1 TN $90^\circ$ configuration

Figure 6 shows a schematic of the TN $90^\circ$  transfective configuration. We can see that one pixel of a normal display is



FIGURE 5 — Prototype of the LTN-TN LCD made at the Center for Display Research (CDR).

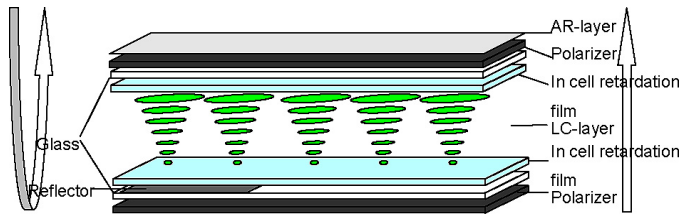


FIGURE 6 — Schematic of TN90° transfective configuration.

divided into two parts. The reflective part is determined by the area of the reflector and usually will be a little smaller than the transmissive part. Two patterned in-cell retardation films are inserted into this configuration. One is fabricated on the front glass and the other, on the rear glass. The two retardation films are patterned by photoalignment technology with a simple two-step exposure. The orientation angle of the retardation film can be adjusted to help optimize the reflective part. But, for the transmissive part, the retardation film is oriented at the same angle as the front and rear polarizer, so they will not have any optical effect on this part. The optimized parameters are shown in Table 2. The angle indicates the counter-clockwise value relative to the horizontal axis.

Figure 7 shows the simulation performance of the TN90° transfective LCD. (a) Spectrum of the reflective part, (b) spectrum of the transmissive part, (c) contrast-ratio distribution of the reflective part, (d) contrast-ratio distribution of the transmissive part, and (e) simulated TVC and RVC. For the reflective part, the reflectance is about 60% of the polarized light, and the maximum contrast is 300 with a 5-V applied voltage. For the transmissive part, the transmittance is 74% of the polarized light, and the maximum contrast is 21 for a 5-V applied voltage considering all reflection from each layer.

## 5 Photoalignment technology

Photoalignment technology was first announced about 20 years ago.<sup>21,22</sup> Since that time, photoalignment has undergone several stages of development from early reports to implementation in real display prototypes. This non-contact alignment method is a direct alternative to rubbing because it allows better uniformity and a high level of control of the liquid-crystal alignment. The later benefit of patterned alignment is becoming popular and is generating a large wave of interest in photoalignment all over the world.<sup>23,24</sup>

The interaction of light with material during photoalignment involves photon absorption. Thus the interaction

TABLE 2 — Optimized parameters of the TN90° configuration.

|                     |             | TN90 transmissive | TN90 reflective |
|---------------------|-------------|-------------------|-----------------|
| Polarizer 1         |             | 0°                | 0°              |
| Compensation film 1 | 90 nm       | 34°               | 0°              |
| LC cell             | cell gap    | 5 μm              | 5 μm            |
|                     | twist angle | 90°               | 90°             |
| Compensation film 2 | 60 nm       | 48°               | 90°             |
| Polarizer 2         |             | 90°               | ////////        |

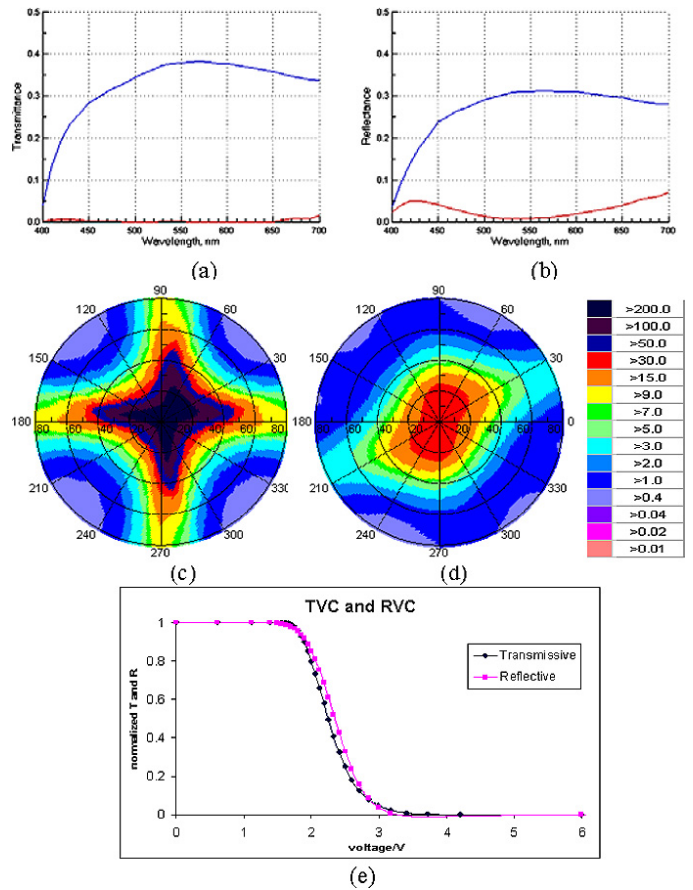


FIGURE 7 — Simulation performance of a TN90° transfective LCD. (a) Spectrum of the reflective part, (b) spectrum of the transmissive part, (c) contrast-ratio distribution of the reflective part, (d) contrast-ratio distribution of the transmissive part, (e) simulated TVC and RVC.

happens on a molecular level, but results in a collective effect on the macroscopically observed parameters, which for the case of liquid-crystal photoalignment are alignment direction, pretilt angle, azimuthal anchoring energy, and polar anchoring energy.<sup>25</sup> The induction mechanisms of the macroscopic parameters of LC photoalignment are molecular in nature and cause anisotropic photo-destruction of the chemical bonds<sup>26</sup> and anisotropic photo-polymerization or statistical reorientation due to photo-isomerization (cis-trans isomers).<sup>27</sup>

In our study, photosensitive sulfuric azo-dye SD1 is used as the photoalignment material, which belongs to the reorientation category, and the diffusion model indicates the rotation of the azo-dye and explains the physics of such rotation under light exposure. The SD1 molecular structure is shown in Fig. 8.

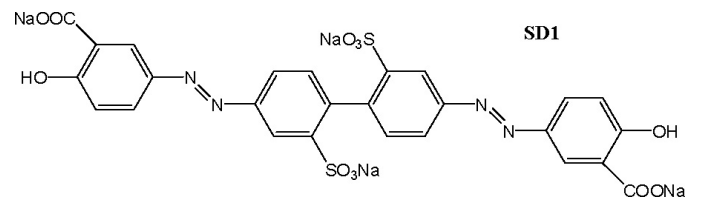
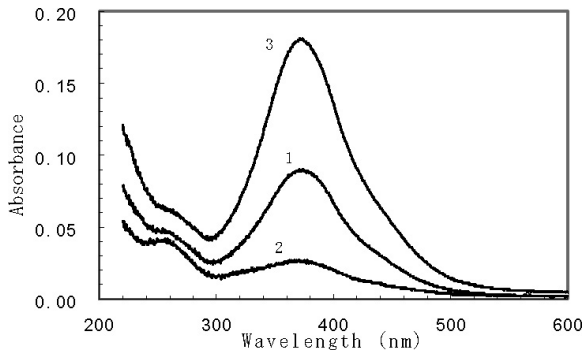


FIGURE 8 — SD1 molecular structure.



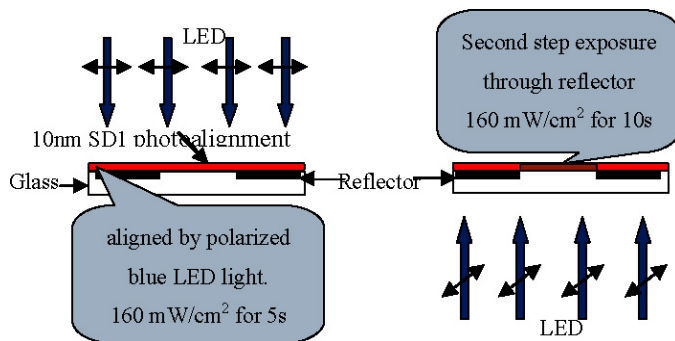
**FIGURE 9** — Absorption spectra of a 100-Å SD1 layer before and after UV light exposure of 1 J/cm<sup>2</sup>.

Figure 9 shows the absorption spectra of a 100-Å SD1 layer before and after UV light exposure of 1 J/cm<sup>2</sup>. Whereas curve 1 was recorded before the UV light exposure, curve 2 was recorded after exposure to parallel linearly polarized UV light; and curve 3, after exposure to perpendicular linearly polarized UV light. A UV spectrophotometer from Perkin Elmer was used for these measurements. The intensity of the absorption spectrum of SD1 decreased after SD1 was exposed to parallel linearly polarized UV light, as shown in curve 2. On the other hand, the intensity of the absorption spectrum increased after SD1 was exposed to perpendicular linearly polarized UV light, as shown in curve 3. Order parameter is defined to express the magnitude of absorption in the parallel and perpendicular directions as follows:

The order parameter  $S$  of the azo-dye chromophores can be expressed as

$$S = \frac{(D_{\parallel} - D_{\perp})}{(D_{\parallel} + 2D_{\perp})},$$

where  $D_{\parallel}$  and  $D_{\perp}$  are the absorption (optical density) of parallel and orthogonal polarized light to the polarization of the activated UV light. The order parameter  $S$  of SD1 is equal to  $-0.4$  at  $\lambda_m = 372$  nm (absorption maximum), which is 80% from its maximum absolute value  $S_m = -0.5$  in our case.



**FIGURE 10** — Fabrication method of patterned alignment layer by photoalignment technology.

## 5.1 Photoaligned patterned alignment layer

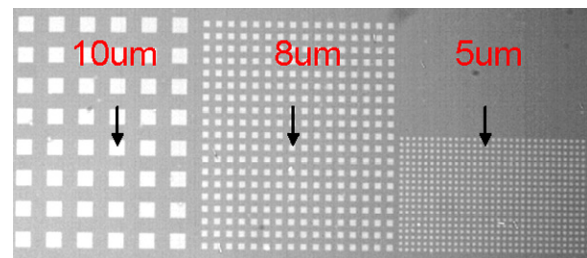
For the dual-mode single-cell-gap transfective approach, different liquid-crystal modes are applied to the reflective and transmissive subpixels. Thus, a patterned alignment layer is required. The conventional rubbing method is not able to produce small-sized domain alignment, but photoalignment provides us with the best solution.

Figure 10 shows the fabrication method for the patterned alignment layer by photoalignment technology. First, we deposit an about 10-nm SD1 layer on the bottom glass surface with a reflector. Then we conducted the first-step exposure using a 440-nm polarized LED source with a power of 160 mW/cm<sup>2</sup> for 5 sec. The SD1 molecule will be aligned to a predetermined direction, which is controlled by the orientation of the LED light polarization. Next, we turn the bottom-glass substrate over and expose the SD1 layer again from the opposite side with the same source for 10 sec. This time, the reflector in the reflective part will block the light, but the SD1 layer of the transmissive part will be totally reoriented to a new direction. By this means, we can fabricate a patterned alignment layer on the glass substrate; thus, an LC cell with dual-domain LC modes can be made. Figure 11 shows the test cell made to find the resolution limit of the photoalignment method. The LC in the square pixel area is made to have a twist angle of 0°, while the LC in the surrounding area is made to have a twist angle of 45°. The minimum domain size that we can achieve in the new experiment is 2 μm, which means the LC transition boundary between two adjacent domains should be smaller than 2 μm. Compared to a 150-μm pixel size, the effect of the transition boundary can be neglected.

## 5.2 Photoaligned patterned in-cell retardation film

For the single-mode single-cell-gap transfective approach, patterned and non-patterned in-cell retardation film is applied to the display to help enhance the performance of both the reflective and transmissive parts. Thus, the flexible in-cell retardation film fabrication method is important for this application. Again, photoalignment provide us with the best solution.

Figure 12 shows the fabrication method of the in cell retardation film by photoalignment technology. First, we



**FIGURE 11** — Dual-mode liquid-crystal domains fabricated by photoalignment technology.

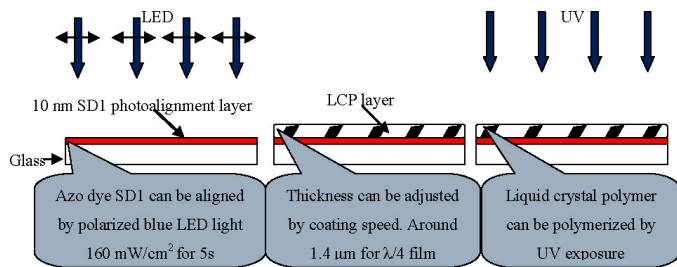


**FIGURE 12** — Fabrication method of the in-cell retardation film by photoalignment technology.

deposited an about 10-nm SD1 layer on the glass substrate. Then we conduct the first-step exposure using the 440-nm polarized LED source with a power of 160 mW/cm<sup>2</sup> for 5 sec. The SD1 molecule will be aligned to a predetermined direction, which is controlled by the orientation of the LED light polarization. Next, we expose the SD1 layer again with a mask under the same LED source for 10 sec. The second-step exposure will totally reorient the SD1 layer in the area, which is not protected by the mask to a new direction. After the patterned alignment layer is made, we deposit the liquid-crystal polymer material, which is liquid crystal but can also be polymerized by UV exposure, on the alignment layer. The LCP material will be aligned by the SD1 layer and thus form a patterned retardation film. One more step of UV exposure will polymerize the LCP layer to produce a solid in-cell retardation film. By this mean, we can fabricate a patterned in-cell retardation film with the required size and thickness, with a precise location.

## 6 Conclusion

In this paper, we reviewed the history of transfective technology and suggested two approaches for single-cell-gap transfective LCDs. One transfective configuration based on the dual-mode single-cell-gap approach has been introduced, as well as another transfective configuration based on the single-mode single-cell-gap approach. Photoalignment technology has been discussed, especially for transfective-LCD applications. Experiments have been performed to demonstrate the performance of the proposed configurations and the fabrication process by photoalignment technology.

## Acknowledgment

This work is supported by grants CERG RPC07/08.EG01, CERG 612409, and CERG 614408.

## Reference

- 1 C. J. Yu *et al.*, *Appl. Phys. Lett.* **85**, 5146 (2004).
- 2 J. B. Bigelow, U.S. Patent No. 4093356 (1978).
- 3 X. Zhu *et al.*, *J. Display Technol.* **1**, 15 (2005).
- 4 H. I. Baek *et al.*, *Proc. IDW '00*, 41 (2000).
- 5 T. B. Jung *et al.*, *Jpn. J. Appl. Phys.* **42**, L464 (2003).
- 6 C. L. Yang, *Jpn. J. Appl. Phys.* **43**, 4273 (2004).
- 7 I. A. Yao *et al.*, *Jpn. J. Appl. Phys.* **45**, 7831 (2006).
- 8 G. S. Lee *et al.*, *Jpn. J. Appl. Phys.* **46**, 289 (2007).
- 9 S. H. Lee *et al.*, *Jpn. J. Appl. Phys.* **42**, L1455 (2003).
- 10 J. H. Song and S. H. Lee, *Jpn. J. Appl. Phys.* **43**, L1130 (2004).
- 11 Y. J. Lim *et al.*, *Jpn. J. Appl. Phys.* **44**, L1532 (2005).
- 12 Y. J. Lee *et al.*, *Jpn. J. Appl. Phys.* **45**, 7827 (2006).
- 13 S. H. Lee *et al.*, *Jpn. J. Appl. Phys.* **42**, 5127 (2003).
- 14 C. J. Yu *et al.*, *Appl. Phys. Lett.* **85**, 5146 (2004).
- 15 Y. J. Lim *et al.*, *Jpn. J. Appl. Phys.* **43**, L972 (2004).
- 16 Y. J. Lim *et al.*, *Jpn. J. Appl. Phys.* **44**, 3080 (2005).
- 17 P. Xu *et al.*, *SID Symposium Digest* **38**, 717 (2007).
- 18 H. Y. Mak *et al.*, *SID Symposium Digest* **39**, (2008).
- 19 V. G. Chigrinov, *Liquid Crystal Devices: Physics and Applications* (Artech-House, Boston, Massachusetts, 1999).
- 20 E. Lueder, *Liquid Crystals Displays* (John Wiley & Sons, London, U.K., 2000).
- 21 K. Ichimura *et al.*, *Langmuir* **4**, 1214 (1988).
- 22 W. M. Gibbons *et al.*, *Nature* **351**, 49 (1991).
- 23 M. Schadt *et al.*, *Jpn. J. Appl. Phys.* **31**, 2155 (1992).
- 24 M. Schadt *et al.*, *Nature* **381**, 212 (1996).
- 25 V. G. Chigrinov *et al.* (Wiley, Chichester, 2008).
- 26 P. J. Martin, "Recent patents on liquid-crystal alignment," *Recent Patents on Mater. Sci.* **1**, 21 (2008).
- 27 J. M. Geary *et al.*, *J. Appl. Phys.* **62**, 4101 (1987).